# Laser-Optical Observation of Chaotic Mixing Structure in a Stirred Vessel

by

Tsukasa MAKINO, Takuya KAISE, Naoto OHMURA and Kunio KATAOKA

Kobe University

Department of Chemical Science and Engineering

Rokkodai-cho, Nada-ku, Kobe 657-8501; Japan

## ABSTRACT

The purpose of the present work is to observe the chaotic mixing structure in a stirred vessel with the aid of flow-visualization using a laser induced fluorescent. Under the laminar flow condition in a stirred vessel, two types of mixing regions were observed, i.e. *active mixing region* (AMR) and *isolated mixing region* (IMR), as shown in figure 1. The IMRs took clearly the form of two toroidal vortices respectively above and below the turbine impeller in the range less than Re = 100. These regions did not interchange much fluid material with the AMR and remained visible for a couple of hours. On the other hand, a good mixing state was observed in the AMR. From the cross sectional view, it has been found that the good mixing in the AMR results from the stretching and folding motion of the turnstile-lobe like regions generated by each stroke of turbine blades. This result indicates that mixing properties in the AMR was strongly dependent on both the secondary circulating flow rate and the passing frequency of turbine blades, which corresponds to the perturbation frequency. Under the same rotational condition, a set of three stable filaments surrounding the core torus of an IMR was found in the case of the six-bladed turbine, while a set of four filaments was found in the case of the four-bladed turbine. Hence it can be considered that these structures depend on the periodical perturbations caused by the rotating turbine blades. In order to observe the inside structure of ring-doughnut-shaped core regions, the unsteady rotation procedure was applied. Another set of filaments was observed to exist inside the core. It has been found that the IMRs had complex multi-structures consisting of various KAM tori. The rotating period of an island $P_i$ and the passing period of turbine blade $P_t$ had a rational relation between them. Furthermore, the rational number of the ratio, $P_i/P_t$, corresponded to the number of islands. These results indicate well the structure complicated with stable/unstable manifolds obtained from the Poincaré-Birkhoff theorem. It can be considered that the geometric structure of the IMRs is controllable depending on the number of blades and the rotational speed of impeller.

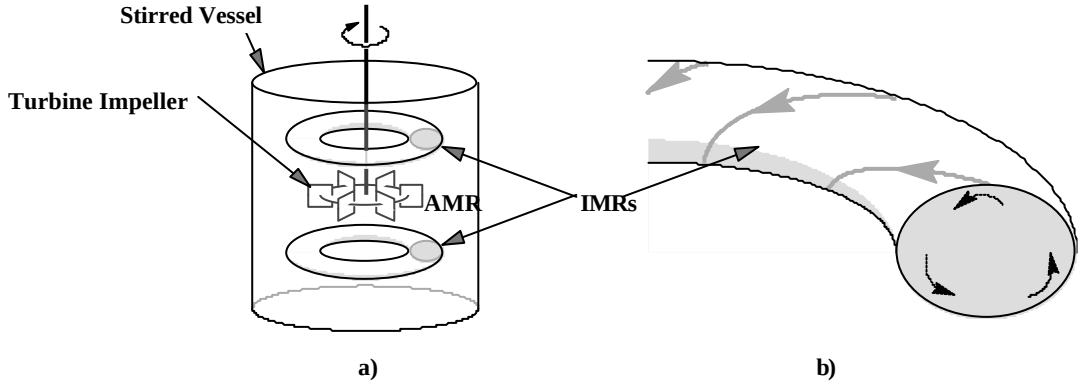


*Fig. 1. Schematic picture of IMR in the stirred vessel*
*a) Schematic picture of AMR and IMRs in the stirred vessel*
*b) Enlarged illustration of IMR*

## 1. INTRODUCTION

Mixing is one of the most important, fundamental operations in industrial chemical processes. Particularly stirred tank reactors are very often used in a wide range of chemical industries. Mixing in a stirred tank reactor is often obliged to be conducted under low Reynolds number conditions, e.g. due to the high viscosity fluids in a polymerization reactor and due to shear-sensitiveness of materials in a bioreactor. These low Reynolds number flow conditions often bring inefficient global mixing which consists of two types of mixing regions, i.e. *active mixing region* (AMR) and *isolated mixing region* (IMR) (Lamberto et al., 1996 and Bresler et al., 1997). As distinct from the IMR, fluid material in the AMR moves fast and interpenetrates very quickly from region to region. Consequently this fluid motion gives a good mixing state in the AMR. On the other hand, the IMRs, which comprise two troidal vortices formed respectively above and below an impeller, do not interchange much fluid material with the AMR. Therefore the IMRs can often serve as a substantial obstacle to global mixing.

Such a non-uniform mixing condition within a stirred tank reactor results in low performance of chemical processes. Hence, every effort has been made to eliminate IMRs effectively. Lamberto et al. (1996) and Yao et al. (1998) demonstrated that the IMRs could be eliminated by using an unsteady rotation method. However, homogeneous mixing does not always bring high performance, depending on the characteristics of chemical processes. Paireau and Tabeling (1997) found experimentally that the overall reactivity under chaotic mixing condition could be enhanced for the second-order reaction as compared to homogeneous mixing. Ouyang et al. (1992) developed a new technique for recovering short-lived chemical intermediate species in an open one-dimensional reaction-diffusion system using a Taylor-Couette flow reactor. Bresler et al. (1997) proposed that the IMR in a chaotic flow could be regarded as a controlled release capsule. They suggested that a possible application of this technique might be a continuous flow reactor where the concentration of one of the reagents should be kept low enough to achieve better conversion or to produce selectively the one preferred among possible reaction products.

In order to take advantage of the non-uniform mixing state for a chemical reaction process, it is necessary to clarify fine structure of IMRs. Since the pioneering work of Aref (1984) and Ottino (1988), the knowledge of chaos in Hamiltonian system has given us a better understanding of two-dimensional laminar mixing, called chaotic mixing. This knowledge is also applicable to three-dimensional laminar flow in a stirred vessel. As Inoue and Hirata (1997) pointed out, it is not sufficient to get the Eulerian information based on local velocity measurement, but to analyze the global trajectories of fluid elements on the basis of Lagrangian observation. In this sense, flow visualization techniques are powerful tools to clarify the chaotic mixing states. The purpose of the present work is, therefore, to observe the chaotic mixing structure in a stirred vessel with the aid of flow visualization using a laser induced fluorescent with a neutralization reaction.

## 2. EXPERIMENTAL

The experimental apparatus consisted of a transparent cylindrical vessel of glass (ID=200mm) and a flat-blade turbine served as a stirrer, as shown in figure 2. The size of these turbines is shown in figure 3. The upper end of the liquid was fixed with a flat plate so that the ratio of the liquid height to the inner diameter of the vessel could be 1. Three kinds of flat-bladed turbines (d = 100 mm) with 3, 4 and 6 blades, respectively, were used. Either of them was installed on the centerline at a distance h = 100 mm (h/D = 0.5) from the bottom of the vessel filled with glycerin. In order to reduce photographic distortion, the cylindrical vessel was mounted into a square vessel of acrylic plates containing glycerin. Two types of experiments were conducted as follow.

Fluorescent neutrally buoyant green dye was used as a passive tracer. The working fluid was initially made basic by adding a small amount of basic solution consisting of 0.5 N NaOH and glycerin. After the turbine reaches a certain rotational speed, a small amount of acidic solution (0.5 N HCl and glycerin) was added at the top of the vessel so as to decolor the green dye due to the neutralization reaction. The IMRs

can be discerned as the regions remaining undecolored in the vessel. The IMRs can be illuminated with the fluorescence induced by a plane sheet of Ar-laser light. The sequential visual data of decoloring process were taken by a digital video camera.

In order to observe fluid motion within the IMRs from a Lagrangian viewpoint, the trajectories of the tracer particles (ion exchanger resin particles, AMBERITE, averaged particle diameter : 1.2 mm) were analyzed by an image processor of computer, as shown in figure 4. The velocity measurement with a laser Doppler velocimeter was made to investigate flow patterns in the vessel.

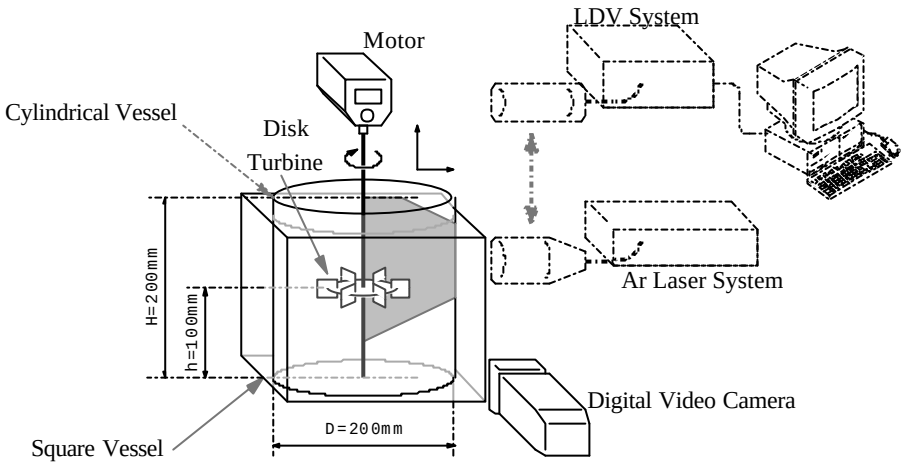


***H/D=1.0***
***d/D=0.5***
***h/D=0.5***

*Fig. 2. Experimental setup*

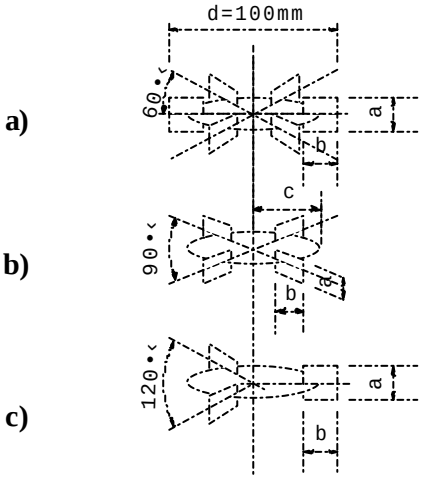


**a)**

**b)**

**c)**

| | a | b | c |
|---|---|---|---|
| 6-bladed | 2.0 | 2.5 | 6.0 |
| 4-bladed | 2.0 | 2.5 | 6.0 |
| 3-bladed | 2.0 | 2.5 | 6.0 |

*Fig. 3. Disk turbines*

*a) Six-bladed turbine*
*b) Four-bladed turbine*
*c) Three-bladed turbine*

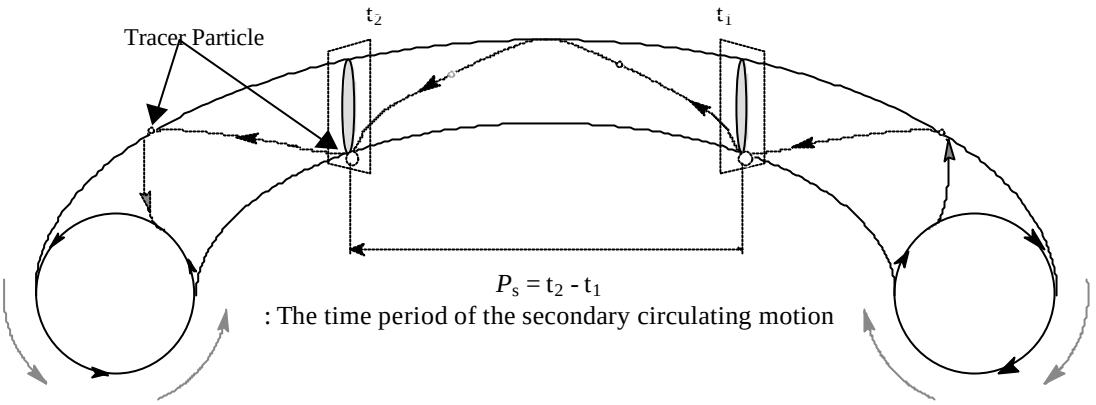


*Fig. 4. Observation of circulating flow motion (Following trajectories of tracer particles)*

## 3. RESULT AND DISCUSSION

### 3.1 Geometric structure of IMR

After the decoloring of AMR was finished, the flow visualization clearly showed the existence of two toroidal regions indicating the IMRs formed on both sides above and below the turbine impeller in the range less than Re (= $nd^2/?$) = 100. Figure 5 shows cross sectional views of the lower isolated mixing region observed with the four-bladed turbine under the condition of Re = 15.6, 28.4, and 37.8, respectively. Under the conditions of this experiment, these regions remained visible for a couple of hours.

In the cases of a)Re=15.6 and b)28.4, some stable islands were observed around the lower torus. Many stable islands whose number could not be identified were observed in the case of a)Re =15.6. With increasing the rotational speed of the impeller, corresponding to b)Re = 28.4, a set of four islands was found around the torus. These islands moved around the core region at a constant period. It can be considered that these structures depend on the rotational speed of the impeller, that is, Re.

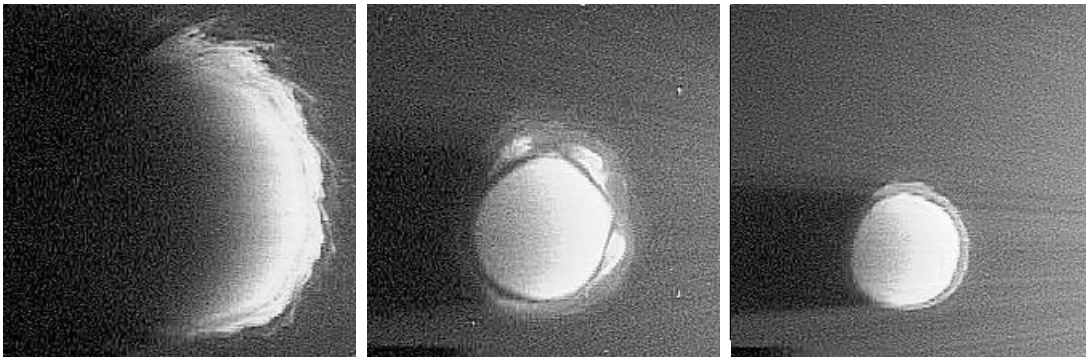

**a)** **b)** **b)**

*Fig. 5. Cross-sectional View of the Lower Isolated Mixing Region Formed with Four-bladed Turbine*
*a) Re= 15.6 : Core region and some stable islands*
*b) Re= 28.4 : Core region and four islands*
*c) Re= 37.8 : Core region*

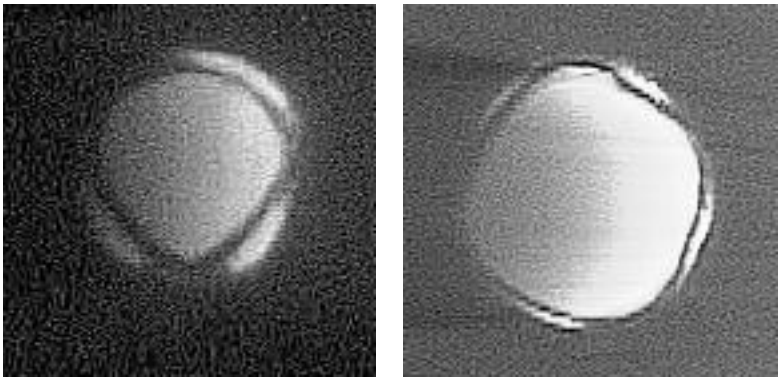

**a)** **b)**

*Fig. 6. Cross-sectional view of the lower isolated mixing region*
*a) Six-bladed turbine : Core region and three islands*
*b) Four-bladed turbine : Core region and four islands*

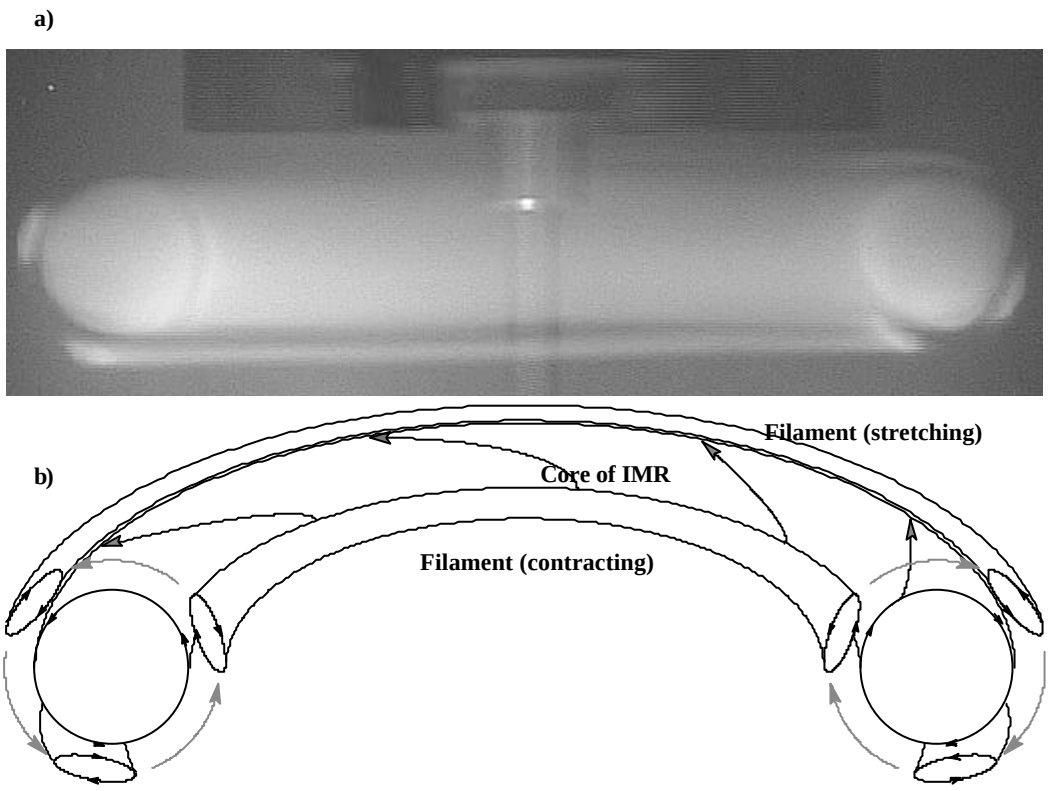


*Fig. 7. Geometrical structure of fluid flow filaments*
*a) Photograph*
*b) Schematic picture*

Figure 6 shows two cross sectional views of the lower isolated mixing region observed with the six-bladed and four-bladed turbines, respectively. A set of three stable islands was observed around the lower torus in the case of three-bladed turbine. When the four-bladed turbine was used, a set of four islands was found around the lower torus. Hence it can be considered that these structures depend not only on the rotational speed of the impeller, but also on the periodical perturbations caused from the blades of the rotating impeller.

Figure 7 shows the global structure of filaments whose cross-sections show the islands. These filaments

form three independent small tori which move around the core of the IMR, iterating stretching and contracting motions. Hence, it has been found that the period of the circulating motion of the cross sectional islands equals to that of the circulating motion of filaments, that is, the secondary circulating motion. Lamberto et al. (1996) presented a clay model of the three-dimensional filament-torus structure observed in their experiment. Their model suggested the filaments wrapping around the core of IMR spirally. In the present work, however, their complex structure could not have been found.

In order to observe the inside structure of doughnut-shaped core regions, the unsteady rotation procedure was applied: Re = 29 ? 0 ? 29. When a set of four filaments was observed outside the torus core region, another set of three filaments was observed inside the core, as shown in figure 8. As a result, it has been found that the isolated mixing regions have complex multi-structures consisting of various KAM tori.

**a)** **b)**

*Fig. 8. Cross-sectional view of multi-structures of isolated mixing region*
*a) Before the unstesdy rotation procedure, Re = 29*
*b) After the unstesdy rotation procedure, Re = 29*

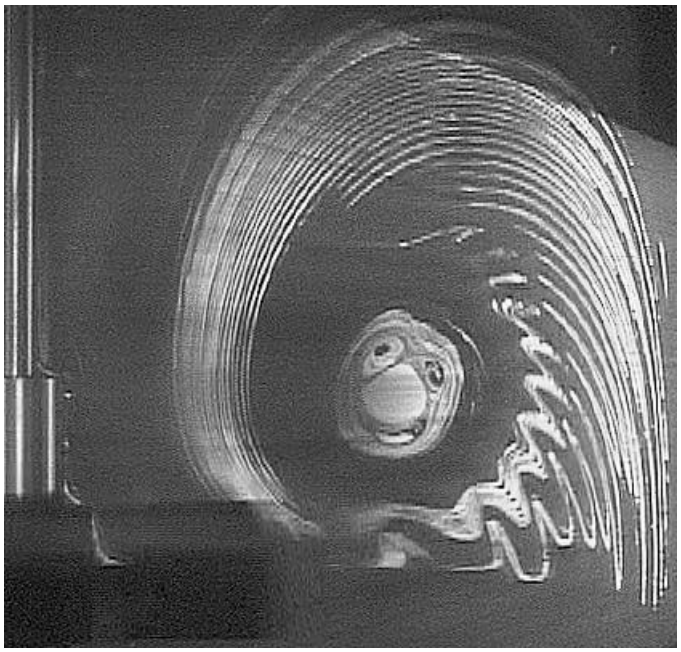

*Fig. 9. Cross-sectional view of active mixing region and isolated mixing region : Re =29*

Figure 9 is a photograph showing IMR and AMR. This figure shows the mixing process in the outer active mixing region quite well. Each stroke of turbine blades generates a turnstile-lobe like structure on the cross section, and the fluid elements within the turnstile-lobe like regions are dominantly exchanged between the upper and lower secondary circulating flow regions. Then the turnstile-lobe like regions are stretched and folded due to the secondary circulating flow. It can be considered that the mixing properties in the AMR depend strongly on both the primary and secondary circulating flow rates and the passing frequency of turbine blades, which corresponds to the perturbation frequency. Consequently, the geometric structure of IMRs also depends on both of them. Hence these effects on the IMR and AMR will be discussed in the following section.

### 3.2 Effect of the impeller rotational speed and the number of blades

Taking our velocity observations into account, it has been found that the center of IMRs corresponds to the center of secondary circulating flow, as shown in figure 10. No significant difference in the location of IMRs can be seen between the six-bladed and four-bladed turbine cases. The central r-z position of cross section of the upper IMR was determined by an image processor, as shown in figure 11. With increasing Reynolds number, the center of the IMR shifts outward and its area becomes small. The same tendency was both experimentally and numerically observed by Lamberto et al. (1996, 1999). It can be considered that the passing frequency of turbine blades is regarded as the periodical perturbation frequency. The higher the Reynolds number, i.e. rotational speed, produces not only the higher the perturbation frequency but also the larger the amplitude of perturbation, i.e. intensity of velocity oscillations. According to Kolmogorov, Anold, and Moser (KAM) theorem (Wiggins, 1990), KAM tori collapse in order from the outer side by increasing the amplitude of perturbation. As described in the previous section, the IMR consists of various KAM tori. Hence the decrease in the area of the IMR with increasing Reynolds number can be attributed to increasing the intensity of velocity oscillations.

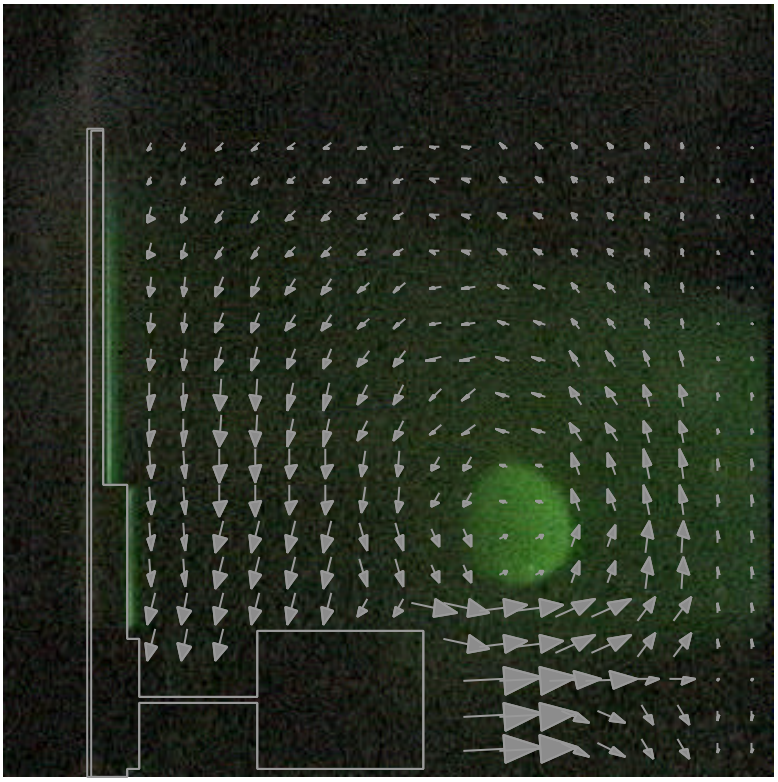

*Fig. 10. Projection of time-averaged velocity vectors on the (r-z) cross section of IMR : Re = 33*

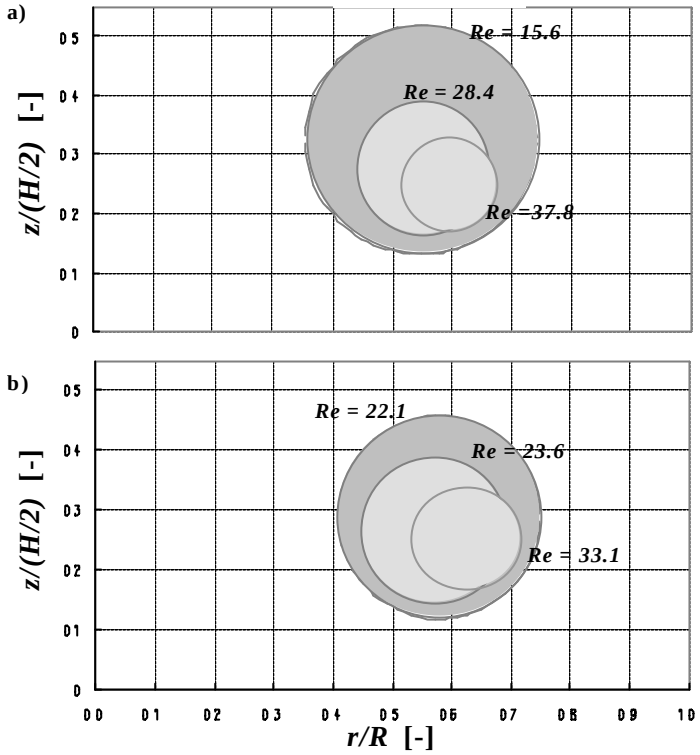


*Fig. 11. Location of cross section of upper IMR*
*a) Four-bladed turbine*
*b) Six-bladed turbine*

By following trajectories of a tracer particle within an IMR, The time period $P_s$ of the secondary circulating motion can be estimated. As shown in figure 12, a good correlation has been found between the time period of secondary circulating flow and the rotational speed of impeller. As a result, it has been found that this circulating flow time period corresponds to the rotation time period of an island around the core region. The behavior of the circulating motion can be described by a power law. As can be seen from figure 12, the exponent of the rotational speed is approximately 2.0. In a Taylor-Couette flow system, such relatively high exponential dependency of mixing properties on rotational speed of inner cylinder was ascertained by our previous work (Ohmura et al., 1997). It can be, therefore, considered that the mixing accompanied by a convective motion at low Reynolds numbers predominantly depends on the circulating motion. Figure 13 shows the ratio of the rotation time period of an island $P_i$ to the passing period of turbine blade $P_t$ at a certain fixed point. It can be seen from figure 13 that $P_i$ and $P_t$ have a rational relation. Furthermore, it has been found that the number of the outer-most islands corresponds to the value of this ratio. These results can well be understood by the Poincaré-Birkhoff theorem in the nonlinear dynamic theory. This theorem says as follows: 1) If the circulation time period on a periodic orbit is $n$ times as long as the perturbation period, $2n$ fixed points generate, where $n$ is integer. 2) Among these $2n$ fixed points, $n$ points are unstable hyperbolic points while the other $n$ points are stable elliptic points. 3) These hyperbolic and elliptic points circularly get lined up by turns. In practice, the unstable hyperbolic fixed points are invisible and the stable elliptic points can only be seen. It can, therefore, be conjectured that the island structures are formed around these stable elliptic fixed points. Consequently, a schematic picture of IMR structure can be depicted, as shown in figure 14. These results imply that the geometric structure of IMRs is controllable by the number of blades and rotational speed of impeller from a viewpoint of the nonlinear dynamic theory.

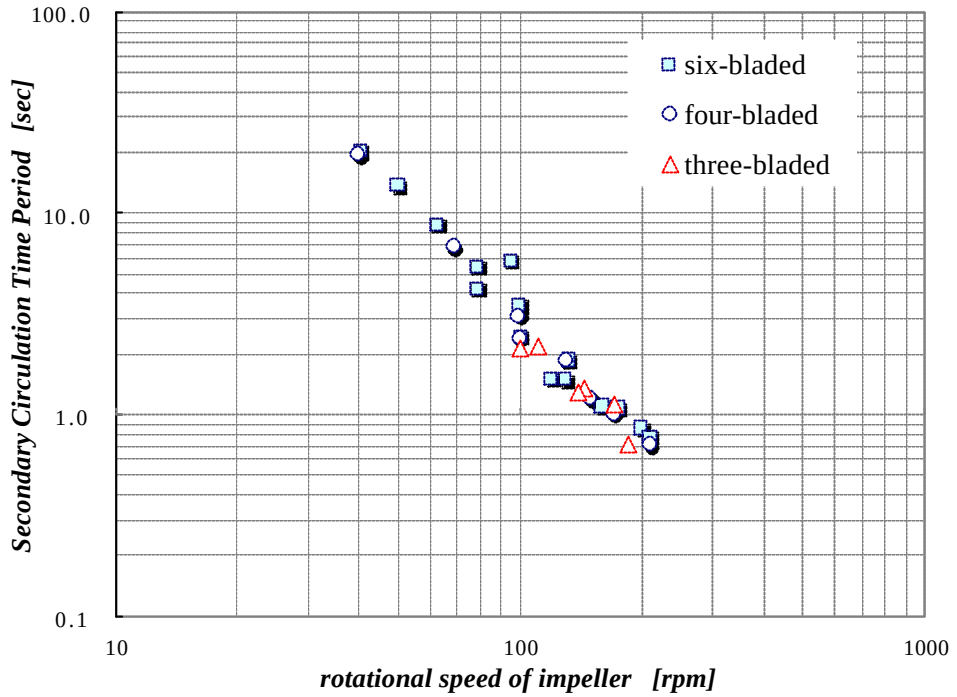


*Fig. 12. Secondary circulation time period against rotational speed of impeller*

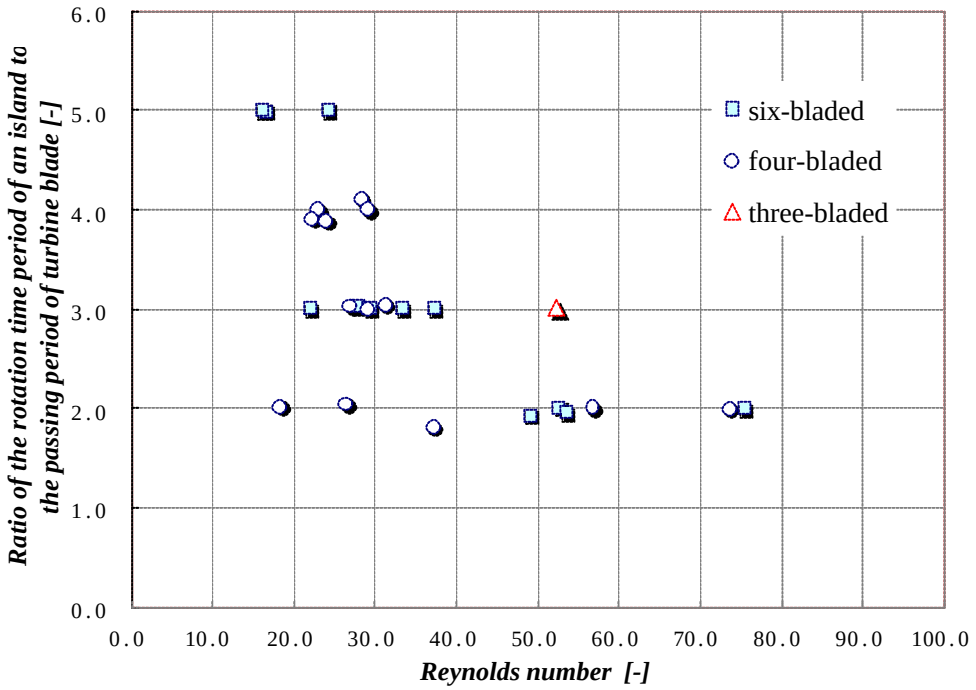


*Fig. 13. Ratio of the rotation time period of an island to the passing period of turbine blade against Reynolds number*

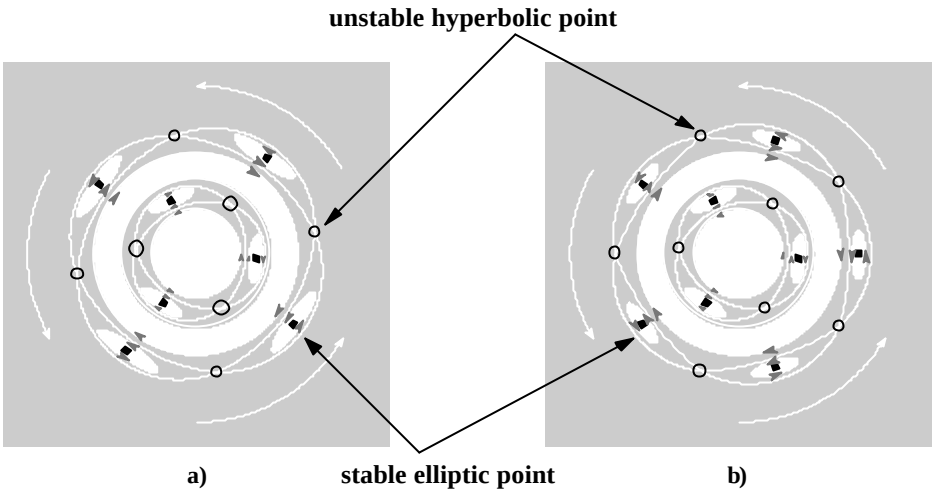


*Fig. 14. Schematic pictures of IMR structure*
*a) 4-3 torus-structure*
*b) 5-3 torus-structure*

## 4. CONCLUSION

The following conclusion has been deduced:

1) Isolated mixing regions have complex multifractal structures consisting of various KAM tori.
2) The geometric structure of IMR depends on periodical perturbations caused by the rotating turbine blades.
3) The central position of IMR is predictable when the information of velocity field is known in detail.
4) The turnstile-lobe like structure can be formed owing to the stroke of turbine blades and the rate of mass exchange between the upper and lower circulating regions can be estimated by this lobe region.
5) The mixing characteristics in AMR depend on both the secondary circulating flow and the passing.
6) With the aid of nonlinear dynamic theory, it might be possible to precisely control the structure of the IMRs by the number of blades and the rotational speed of impeller.

**Acknowledgement**
The authors wish to thank Messrs. T. Takigawa and T. Yoshimura for experimental support. This research was financially supported by a Grand-in-Aid for Encouragement of Young Scienticts (no. 10750547) from the ministry of Education, Science, Sports and Culture of Japan. This research belongs to the "Methodology for Emergent Synthesis" Project (project number 96P00702) in the "Research for the Future" Program of JSPS.

## NOTATION

*d* impeller diameter, m
*D* diameter of vessel, m
*h* height of vessel, m
*n* rotational speed, 1/s
*Re* Reynolds number (= *n*? $d^2$/?), -

Greek letter
? kinematic viscosity, $m^2$/s

## REFERENCES


Aref, H. (1984), "Stirring by Chaotic Advection", J. Fluid. Mech., 143, pp. 1-21

Bresler, L., Shinbrot, T., Metcalfe, G. and Ottino, M. J. (1997). "Isolated Mixing Regions: Origin, Robustness and Control", Chem. Eng. Sci., **52**, pp. 1623-1636

Inoue, Y. and Hirata, Y. (1997), "Intercellular Chaotic Mixing by Lagrangian Turbulence", Proc. 10th Int. Symp. On Transport Phenomena in Thermal Science and Process Engineering, Kyoto November 30 – December 3, Vol 1, pp. 227-232

Lamberto, D. J., Muzzio, F. J., Swanson, P. D. and Tonkovich, A. L. (1996), "Using Time-Dependent RPM to Enhance Mixing in Stirred Vessels", Chem. Eng. Sci., **51**, pp. 733-741

Lamberto, D. J., Alvarez, M. M. and Muzzio, F. J. (1999), "Experimental and Computational Investigation of Laminar Flow Structure in a Stirred Tank", Chem. Eng. Sci.,**54**, pp. 919-942

Ohmura, N., Kataoka, K., Shibata, Y. and Makino, T. (1997), "Effective Mass Diffusion over Cell Boundaries in a Taylor-Couette Flow System", Chem. Eng. Sci.,**52**, pp. 1757-1765

Ottino, J. M., Leong, C. W., Rising, H. and Swanson, P. D. (1988), "Morphological Structures Produced by Mixing in Chaotic Flows", Nature, 333, pp. 419-425

Ouyang, Q., Swinney, H. L., Roux, J. C., De Kepper, P. and Boissonade, J. (1992), "Recovery of Short-lived Chemical Species in a Couette Flow Reactor", A.I.Ch.E. J., **38**, pp. 502-510

Paireau, O. and Tabeling, P. (1997), "Enhancement of the Reactivity by Chaotic Mixing", Phys. Rev. E, **56**, pp. 2287-2290

Wiggins, S. (1990), "Introduction to Applied Nonlinear Dynamical Systems and Chaos",Springer-Uerlag, New York, USA

Yao, W. G., Sato, H., Takahashi, K. and Koyama, K. (1998), "Mixing Performance Experiments in Impeller Stirred Tanks Subjected to Unsteady Rotational Speeds", Chem. Eng. Sci., **53**, pp. 3031-3040